POLITECNICO DI TORINO
Repository ISTITUZIONALE

Impacts and StateDependence of AMOC Weakening in a Warming Climate

Original
Impacts and StateDependence of AMOC Weakening in a Warming Climate / Bellomo, K., Mehling, O.. - In: GEOPHYSICAL RESEARCH LETTERS. - ISSN 0094-8276. - 51:10(2024). [10.1029/2023gl107624]

Availability:
This version is available at: 11583/2993060 since: 2024-10-04T10:00:57Z

Publisher:
AMER GEOPHYSICAL UNION

Published
DOI:10.1029/2023gl107624

Terms of use:

This article is made available under terms and conditions as specified in the corresponding bibliographic description in the repository

Publisher copyright
AGU

Da definire

(Article begins on next page)

27 November 2026

Check for updates

AGU ADVANCING EARTH AND SPACE SCIENCES

Geophysical Research Letters

RESEARCH LETTER
10.1029/2023GL107624

Impacts and State-Dependence of AMOC Weakening in a Warming Climate

Katinka Bellomo[1,2] and **Oliver Mehling**[1]

[1]Department of Environment, Land and Infrastructure Engineering, Polytechnic University of Turin, Turin, Italy, [2]National Research Council of Italy, Institute of Atmospheric Sciences and Climate, Turin, Italy

Abstract All climate models project a weakening of the Atlantic Meridional Overturning Circulation (AMOC) strength in response to greenhouse gas forcing. However, the climate impacts of the AMOC decline alone cannot be isolated from other drivers of climate change using existing Coupled Model Intercomparison Project simulations. To address this issue, we conduct idealized experiments using the EC-Earth3 climate model. We compare an abrupt $4\times CO_2$ simulation with the same experiment, except we artificially fix the AMOC strength at preindustrial levels. With this design, we can formally attribute differences in climate change impacts between these two experiments to the AMOC decline. In addition, we quantify the state-dependence of AMOC impacts by comparing the aforementioned experiments with a preindustrial simulation in which we artificially reduce the AMOC strength. Our findings demonstrate that AMOC decline impacts are state-dependent, thus understanding AMOC impacts on future climate change requires targeted model experiments.

Plain Language Summary Climate models predict that the Atlantic Ocean's major circulation system, known as the Atlantic Meridional Overturning Circulation (AMOC), will weaken during the 21st century. This weakening could have significant impacts on the climate. However, it is challenging to isolate the AMOC's effects because other factors, such as rising greenhouse gas levels, also affect the climate. To better understand the AMOC's role, in this study we use a climate model to conduct numerical experiments. We compare a simulation of the preindustrial climate with one in which we artificially decrease the strength of the AMOC. Then, we compare the preindustrial climate with two forced simulations: one with a fourfold increase in atmospheric carbon dioxide, where the AMOC weakens as expected, and another where we keep the AMOC at its preindustrial strength despite higher CO_2 levels. By comparing these experiments, we determine that the impacts of an AMOC decline depend on the background climate state. This research demonstrates that ad-hoc model experiments are needed to understand the impacts of a weakened AMOC in a changing climate.

Key Points:

- We present new idealized experiments to assess the influence of a weakened Atlantic Meridional Overturning Circulation (AMOC) on future climate change
- We use the EC-Earth3 climate model to carry out experiments imposing abrupt $4\times CO_2$ forcing but fixing the AMOC strength, and then we compare them with preindustrial water hosing experiments
- We find that AMOC impacts on temperature and precipitation depend on the background climate state

Supporting Information:

Supporting Information may be found in the online version of this article.

Correspondence to:

K. Bellomo,
katinka.bellomo@polito.it

Citation:

Bellomo, K., & Mehling, O. (2024). Impacts and state-dependence of AMOC weakening in a warming climate. *Geophysical Research Letters*, *51*, e2023GL107624. https://doi.org/10.1029/2023GL107624

Received 5 DEC 2023
Accepted 16 APR 2024

Author Contributions:

Conceptualization: Katinka Bellomo
Formal analysis: Katinka Bellomo, Oliver Mehling
Funding acquisition: Katinka Bellomo
Investigation: Katinka Bellomo, Oliver Mehling
Methodology: Katinka Bellomo, Oliver Mehling
Project administration: Katinka Bellomo
Resources: Katinka Bellomo
Supervision: Katinka Bellomo
Visualization: Katinka Bellomo, Oliver Mehling

© 2024. The Authors.
This is an open access article under the terms of the Creative Commons Attribution-NonCommercial-NoDerivs License, which permits use and distribution in any medium, provided the original work is properly cited, the use is non-commercial and no modifications or adaptations are made.

1. Introduction

The Atlantic Meridional Overturning Circulation (AMOC) plays a unique role in the climate system by carrying an excess heat of about 0.5 PW across the equator into the North Atlantic (e.g., Buckley & Marshall, 2016; Srokosz et al., 2021; Trenberth et al., 2019). This inter-hemispheric heat transport imbalance is believed to create an asymmetry in the distribution of temperature and precipitation. Specifically, the AMOC is thought to be responsible for the Northern Hemisphere (NH) to be ∼1°C warmer than the Southern Hemisphere (SH) (Feulner et al., 2013) and for shifting the latitude of the Inter-tropical Convergence Zone (ITCZ) north of the equator to ∼5° N (Frierson et al., 2013; Marshall et al., 2014).

Changes in AMOC strength influence North Atlantic Sea Surface Temperature (SST) variability on multiple timescales (Zhang et al., 2019), and AMOC changes have been invoked to explain abrupt climate change and glacial-interglacial transitions (e.g., Lynch-Stieglitz, 2017; Malmierca-Vallet & Sime, 2023; Moffa-Sanchez et al., 2019). There are contrasting views on whether a significant weakening of the AMOC can already be detected in the present-day climate compared to the last millennium (e.g., Caesar et al., 2021; Kilbourne et al., 2022; Latif et al., 2022; Rahmstorf et al., 2015; Worthington et al., 2021). However, all future projections from the most recent Coupled Model Intercomparison Project Phase 6 (CMIP6) show a steady decline in AMOC strength throughout the 21st century (Weijer et al., 2020). The consistent AMOC decline in future projections can physically be explained by increased ocean stratification and upper ocean warming, which inhibit the thermo-haline circulation (Fox-Kemper et al., 2021).

Writing – original draft: Katinka Bellomo
Writing – review & editing: Katinka Bellomo, Oliver Mehling

The effects of this AMOC weakening on the global climate compete with other direct and indirect effects of greenhouse gas forcing. Because the uncertainty in the projected magnitude of AMOC weakening is large (Bellomo et al., 2021; Reintges et al., 2017; Weijer et al., 2020), several strategies have been proposed to assess the climatic impacts due to an AMOC decline. One well-established approach is that of the "water hosing" experiments, in which the AMOC is artificially weakened through the release of a freshwater anomaly in regions of deep-water formation (e.g., Stouffer et al., 2006; Jackson et al., 2023 and references therein). Previous studies show that an abrupt decline in AMOC strength leads to a cooling in the NH, in particular in the North Atlantic and the Arctic. This enhanced equator-to-pole surface temperature gradient leads to stronger westerlies in the mid-latitudes and an eastward elongation of the jet stream in the North Atlantic (e.g., Brayshaw et al., 2009; Woollings et al., 2012), with consequences on blocking and cold spells in Eurasia (Meccia et al., 2024). Well-known impacts of an AMOC decline also include a widespread reduction in precipitation throughout the NH (e.g., Bellomo et al., 2023; Jackson et al., 2015) and a southward migration of the ITCZ (e.g., Kang et al., 2008; Zhang & Delworth, 2005). However, water hosing experiments are typically initialized from a pre-industrial climate, and it is not clear whether the impacts of the AMOC decline in those experiments can be generalized to explain the impacts of a weakened AMOC in a much warmer climate. Indeed, in the paleoclimate context (Kageyama et al., 2013) and idealized model simulations (Vellinga & Wood, 2008), it has been suggested that at least some impacts of an AMOC decline could be state-dependent.

Vellinga and Wood (2008) with an earlier generation model assessed the impacts of an AMOC shutdown in a scenario of the 21st century climate change, forcing the AMOC to stop by adding a freshwater anomaly using the "water hosing" experimental design. With this design, they were able to assess the impacts of a potential AMOC shutdown in the 21st century. More recently, using the CCSM4 climate model, Liu et al. (2020) assessed the effects of an AMOC decline alone by comparing the impacts of a weakened AMOC in the Representative Concentration Pathway 8.5 scenario with another experiment in which they artificially stabilized the AMOC at historical levels. To date, there are no other studies that employ model experiments to address the impacts of a weakening AMOC on future climate change using other CMIP5 or newer model generations.

Here, we perform climate model experiments in which we stabilize the AMOC strength, but with prescribed $4\times CO_2$ forcing. This corresponds approximately to CO_2 levels by the end of the 21st century in the highest-emission scenario considered by the Intergovernmental Panel on Climate Change (IPCC; Chen et al., 2021). Differently from previous studies, we use a CMIP6 model (EC-Earth3) at higher resolution, and our fixed AMOC experiments are designed to obtain a stable AMOC strength for about 100 years. By comparing these new experiments with the water hosing ones, we are able to formally investigate the mean climate state-dependence of AMOC impacts.

2. Data and Methodology

2.1. Model Experiments With EC-Earth3

We analyze model experiments with state-of-the-art coupled climate model EC-Earth3 (Döscher et al., 2022), which participates in CMIP6 (Eyring et al., 2016). EC-Earth3 includes the IFS cy36r4 atmospheric model, the land-surface scheme H-TESSEL (Balsamo et al., 2009), the NEMO 3.6 ocean model (Madec, 2015) and the LIM3 sea-ice component (Rousset et al., 2015). The OASIS3-MCT version 3.0 coupler exchanges fields between the components (Craig et al., 2017). In all of the experiments, EC-Earth3 has a horizontal resolution of ∼80 km (T255) for the atmosphere and ∼100 km (1°) for the ocean, with a grid refinement to 1/3° in the tropical ocean. The vertical levels are 91 for the atmosphere and 75 for the ocean.

Our control climate is taken from the preindustrial control ("picontrol") experiment from the CMIP6 archive (ensemble member r1i1p1f1) and is 500 years long. All variability in this experiment is internally driven since external radiative forcings are kept fixed at preindustrial levels (CO_2 is at ∼284 ppm). We investigate the impacts of greenhouse gas forcing by analyzing the abrupt-$4\times CO_2$ ("$4\times CO_2$") experiment, also taken from the CMIP6 archive (ensemble member r8i1p1f1). The $4\times CO_2$ experiment is initialized from the picontrol experiment and is forced with a fixed CO_2 concentration of four times the preindustrial level for 150 years (Eyring et al., 2016).

In addition, we carry out two types of experiments: the first one is a "water hosing" experiment, and is described in Bellomo et al. (2023). The water hosing experiment is integrated for 140 years adding a uniform negative virtual salinity flux equivalent to −0.3 Sv (1 Sv = 10^6 m^3/s) poleward of 50°N in the Atlantic and Arctic Oceans.

19448007, 2024, 10, Downloaded from https://agupubs.onlinelibrary.wiley.com/doi/10.1029/2023GL107624 by Politecnico Di Torino Sist. Bibl Del Polit Di Torino, Wiley Online Library on [13/05/2024]. See the Terms and Conditions (https://onlinelibrary.wiley.com/terms-and-conditions) on Wiley Online Library for rules of use; OA articles are governed by the applicable Creative Commons License

19448007, 2024, 10, Downloaded from https://agupubs.onlinelibrary.wiley.com/doi/10.1029/2023GL107624 by Politecnico Di Torino Sist. Bibl Del Polit Di Torino, Wiley Online Library on [13/05/2024]. See the Terms and Conditions (https://onlinelibrary.wiley.com/terms-and-conditions) on Wiley Online Library for rules of use; OA articles are governed by the applicable Creative Commons License

Then, the hosing is halted and the model is left to freely evolve for an additional 70 years. As in Bellomo et al. (2023), here we analyze the 60 years (model years 100–159) in which the AMOC strength is less than half the strength of the preindustrial mean. The second type of experiment is identical to the abrupt-4×CO_2, including initial conditions, but we artificially keep the AMOC strength at values comparable to the preindustrial. In this experiment, we also add a uniform virtual salinity flux poleward of 50°N in the Atlantic and Arctic Oceans as in Bellomo et al. (2023), but while in the water hosing experiment we apply a negative virtual salinity flux to decrease the strength of the AMOC, here we apply a positive virtual salinity flux to counterbalance the weakening of the AMOC induced by the 4×CO_2 forcing. We run three ensemble members, which are identical in the setup and initial conditions but differ in the amount of the virtual salinity flux. The three ensemble members will be referred to as "4×CO_2 + 0.4 Sv", "4×CO_2 + 0.5 Sv", and "4×CO_2 + 0.6 Sv." In many cases, we will show the ensemble mean of the three members to better isolate the forced response from internal variability. We will refer to the ensemble mean as the "fixed AMOC" experiment in the text and figures.

Table S1 in Supporting Information S1 provides a short summary of these experiments. We note that in the virtual salinity flux experiments, total ocean salinity is conserved by applying a correction elsewhere in the ocean, and the ocean volume does not change. We point the reader to Bellomo et al. (2023) for additional specifications on this experimental setup.

2.2. Data Analysis and Statistical Methods

For the picontrol experiment, we present long-term means of the entire 500-year simulation. For the 4×CO_2 experiments, we select model years 50–150 in which the AMOC is in quasi-equilibrium. The impacts of AMOC weakening after CO_2 quadrupling are obtained by subtracting the mean of the positive virtual salinity flux experiments from the abrupt-4×CO_2 run in which the AMOC weakens. To test whether significant differences emerge from internal variability, we use a two-tailed Welch's *t*-test allowing for different variances and sample sizes at the 90% significance level. Areas where differences are not statistically significant are indicated with stippling in the figures.

We define the "state-dependence" as the deviation from the null hypothesis that the impacts of AMOC weakening are invariant to the background climate state: for example, the effects of surface warming due to CO_2 quadrupling and those of AMOC weakening are simply additive. We assess state-dependence by comparing the impacts of AMOC weakening under 4×CO_2 as described above (i.e., fixed AMOC minus 4×CO_2), from the impacts of AMOC weakening obtained from the water hosing experiment in pre-industrial climate (i.e., water hosing minus picontrol). We note that in the water hosing experiment the average AMOC strength in the years considered is 10.2 Sv weaker than in the picontrol, but the difference in AMOC strength between the fixed AMOC and 4×CO_2 experiments is 8.2 Sv. Hence, we linearly scale the extrapolated AMOC impacts from the water hosing experiment by a factor of 0.8 so that they would be fully comparable with the fixed AMOC minus 4×CO_2 results if the effects of a weakened AMOC did not depend on the background climate state. We believe that the scaling does not affect our main conclusions since results are also similar when comparing the water hosing experiment (−10.2 Sv relative to preindustrial) with the 4×CO_2 + 0.6 Sv (−9.7 Sv relative to 4×CO_2), although some regional impacts may depend on the exact amount of AMOC weakening.

3. Results

3.1. AMOC

Figure 1 shows timeseries of annual mean maximum AMOC strength at 26.5°N in the model experiments. For the picontrol experiment, we show the long-term mean as a horizontal thick black line, while the gray shading spans plus and minus 1.5 standard deviations from the mean. This is meant to represent the mean AMOC strength in the picontrol experiment plus an estimate of its internal variability. The red curve shows the AMOC strength in the 4×CO_2 experiment, while the three blue curves are the three positive virtual salinity flux experiments. As expected, the positive virtual salinity flux counterbalances the 4×CO_2 forcing, resulting in an AMOC strength for the three experiments that spans the range of internal variability estimated from the picontrol run. The average value of AMOC strength in the picontrol is 17.8 ± 2.4 Sv, while it is 17.2, 18.8, and 20.2 Sv over model years 50–150 for the 4×CO_2 + 0.4 Sv, 4×CO_2 + 0.5 Sv, and 4×CO_2 + 0.6 Sv experiments, respectively. In the 4×CO_2 experiment, the AMOC strength weakens to an average of 10.2 Sv, which corresponds to a 43% reduction compared to preindustrial levels.

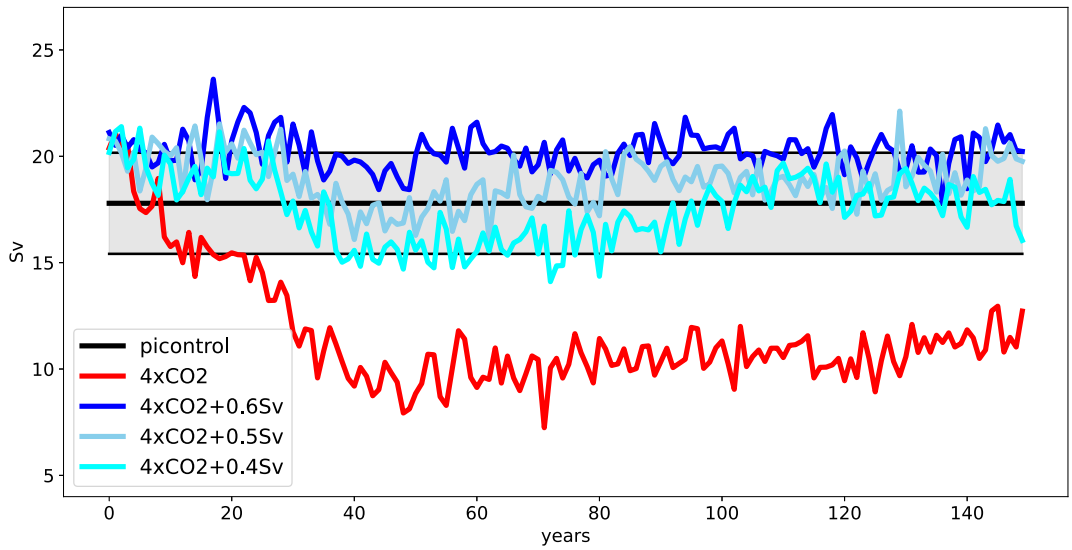


Figure 1. Atlantic Meridional Overturning Circulation strength at 26.5°N. The timeseries are calculated as the annual mean maximum of the mass overturning streamfunction in the Atlantic sector below 500 m. The picontrol is represented as the long-term mean (thick black line) and the gray band spans plus and minus 1.5 standard deviations for an estimate of internal variability. The other curves are colored according to the legend.

The AMOC streamfunction and mixed layer depth (MLD) are shown in Figures S1–S3 in Supporting Information S1. Compared to the picontrol, the streamfunction weakens south of 60°N in the 4×CO_2 but strengthens northward (Figure S1 in Supporting Information S1). In the three positive virtual salinity flux experiments, in addition to an overall strengthening compared to the 4×CO_2 run, we also see a northward extension of the AMOC streamfunction (Figure S2 in Supporting Information S1). The streamfunction for the water hosing experiment features an overall weakening at all latitudes from preindustrial values (Figure S1 in Supporting Information S1). An examination of changes in MLD (Figure S3 in Supporting Information S1) shows more convection in the Arctic due to the 4×CO_2 forcing (Figure S3a in Supporting Information S1). With the addition of virtual salinity flux, there is enhanced deep water formation in the Labrador Sea compared to picontrol and 4×CO_2 forcing (Figure S3b in Supporting Information S1). Thus, the AMOC streamfunction and the MLD are different than in the preindustrial climate because the virtual salinity flux cannot undo the effects of greenhouse gases. The differences in these two variables seem to be related to changes in sea ice concentration (cf. Figure S6 in Supporting Information S1), and these differences are due to the 4×CO_2 forcing despite the counterbalancing effect of the virtual salinity flux and strengthened AMOC.

3.2. Temperature

Figure 2 shows annual mean changes in near-surface air temperature. Boreal winter (DJF) and summer (JJA) changes may be found in supplemental Figure S4 in Supporting Information S1. Figure 2a shows the difference between the 4×CO_2 and picontrol experiments: the response shares some well-known characteristics of greenhouse gas forced climate change as seen in other models, such as polar amplification and land-sea warming contrast. Figure 2b shows the difference between fixed AMOC (i.e., average of the three positive virtual salinity flux experiments) and the picontrol run. While some large-scale features of temperature change largely resemble Figure 2a, Figure 2c (computed as panel a minus b) shows that there are some important differences. The weaker AMOC in the 4×CO_2 experiment reduces the warming in the entire NH compared to fixed AMOC, while it increases the warming in the SH. The differences are almost everywhere statistically significant in Figure 2c, except over the stippled areas, which are mostly located over the SH tropics and the Southern Ocean. The reduced warming displays a horseshoe pattern similar to the AMV (e.g., Bellomo et al., 2018), and is present both in summer and winter, but is larger in winter (Figure S4a in Supporting Information S1). In summer (Figure S4b in Supporting Information S1), a weaker AMOC results in enhanced warming in Africa north of the equator and over the Sahel. The enhanced warming over this region in summer is seen in the annual mean change (Figure 2c).

19448007, 2024, 10, Downloaded from https://agupubs.onlinelibrary.wiley.com/doi/10.1029/2023GL107624 by Politecnico Di Torino Sist. Bibl Del Polit Di Torino, Wiley Online Library on [13/05/2024]. See the Terms and Conditions (https://onlinelibrary.wiley.com/terms-and-conditions) on Wiley Online Library for rules of use; OA articles are governed by the applicable Creative Commons License

10.1029/2023GL107624

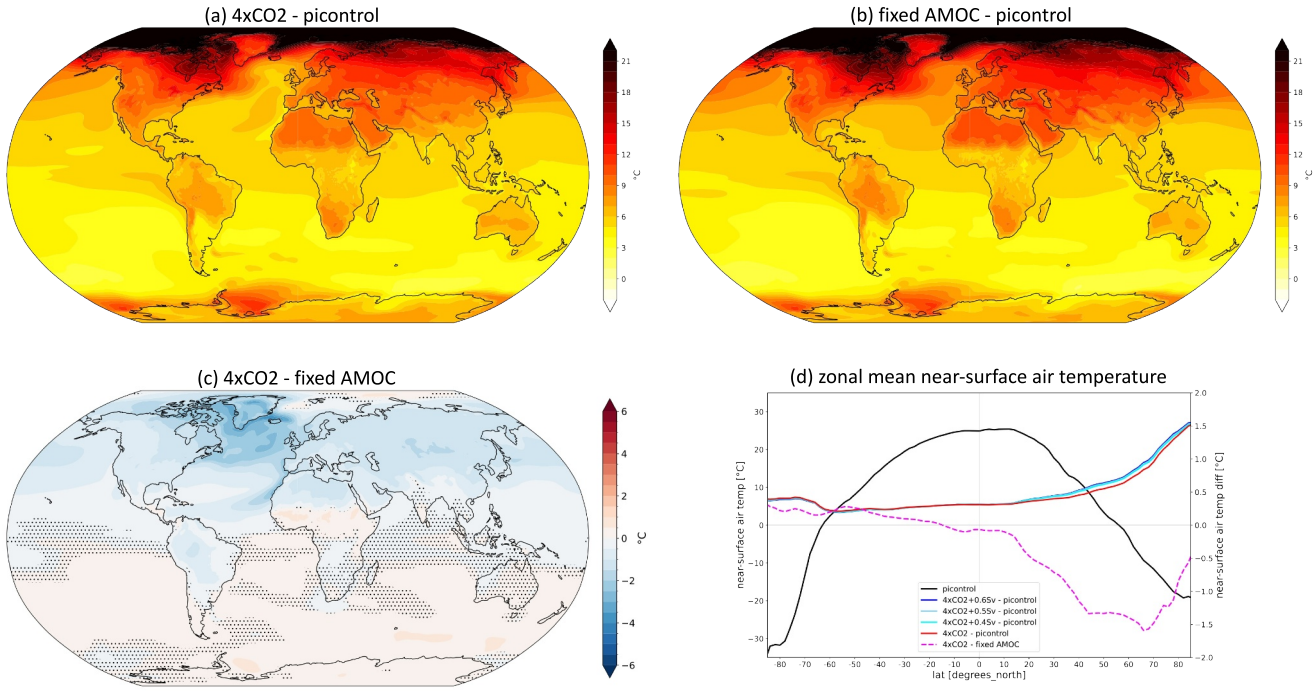


Figure 2. Near-surface air temperature. Maps show the changes in near-surface air temperature between $4\times CO_2$ and picontrol (panel a), fixed Atlantic Meridional Overturning Circulation (AMOC) and picontrol (panel b), $4\times CO_2$ and fixed AMOC (panel c). Stippling in panel (c) shows areas where the difference is not statistically significant. Panel (d) shows zonal mean near-surface air temperature: the black curve represents the picontrol climatology (refers to left hand side *y*-axis); the four solid curves represent changes from the picontrol (see legend); the dashed magenta curve represents the differences between the $4\times CO_2$ and fixed AMOC experiments.

While the AMOC weakening has a significant effect on globally averaged temperature change (−0.3°C, $p < 0.001$), we find that the effect on net radiation imbalance at the top-of-atmosphere is small and not significant (+0.08 W/m^2, $p = 0.14$). In certain regions the cooling effect of the AMOC decline is larger: for example, over the North Atlantic the effect is −1°C, and over the Subpolar North Atlantic (SPNA) is as large as −2.4°C. Figure 2d further shows the zonal mean near-surface air temperature change in the experiments. The difference between fixed AMOC experiments and the $4\times CO_2$ (magenta curve) is most pronounced in the band 50°N–70°N, where the cooling effect of the AMOC exceeds 1°C.

3.3. Precipitation

In Figure 3 we show the impact of a weaker AMOC on precipitation. Figure 3a shows the difference in annual mean precipitation between the $4\times CO_2$ and the picontrol. Figure 3b is the same as Figure 3a but for the difference between the fixed AMOC and the picontrol. Here too, large-scale features of precipitation change in response to CO_2 quadrupling are similar between the $4\times CO_2$ and fixed AMOC experiments (Figures 3a and 3b). However, as a consequence of an AMOC decline (Figure 3c) we note widespread drying in the North Atlantic, precipitation increase over the Arctic ocean, small but significant precipitation decrease over large parts of Eurasia, and a southward shift of the ITCZ in all oceans. Figure S5 in Supporting Information S1 further shows that changes in the North Atlantic region and in the Arctic and Eurasia, as well as equatorial Pacific precipitation impacts, occur mainly in boreal winter (DJF), while the southward ITCZ shift in the Atlantic Ocean occurs mainly in boreal summer (JJA).

Figure 3d shows zonal mean precipitation. Compared to the climatology (black curve, left hand side *y*-axis), precipitation change in the $4\times CO_2$ experiment displays a narrowing of tropical precipitation and expansion of the subtropical dry zones, while the mid-to-high latitudes get wetter in both hemispheres. On the other hand, the three positive virtual salinity flux experiments all exhibit a southward shift of the ITCZ and a dryer NH. Similar to Figure 2d, we note that differences in precipitation change between the three targeted experiments are much smaller compared to differences between their ensemble mean and the $4\times CO_2$ simulation.

19448007, 2024, 10, Downloaded from https://agupubs.onlinelibrary.wiley.com/doi/10.1029/2023GL107624 by Politecnico Di Torino Sist. Bibl Del Polit Di Torino, Wiley Online Library on [13/05/2024]. See the Terms and Conditions (https://onlinelibrary.wiley.com/terms-and-conditions) on Wiley Online Library for rules of use; OA articles are governed by the applicable Creative Commons License

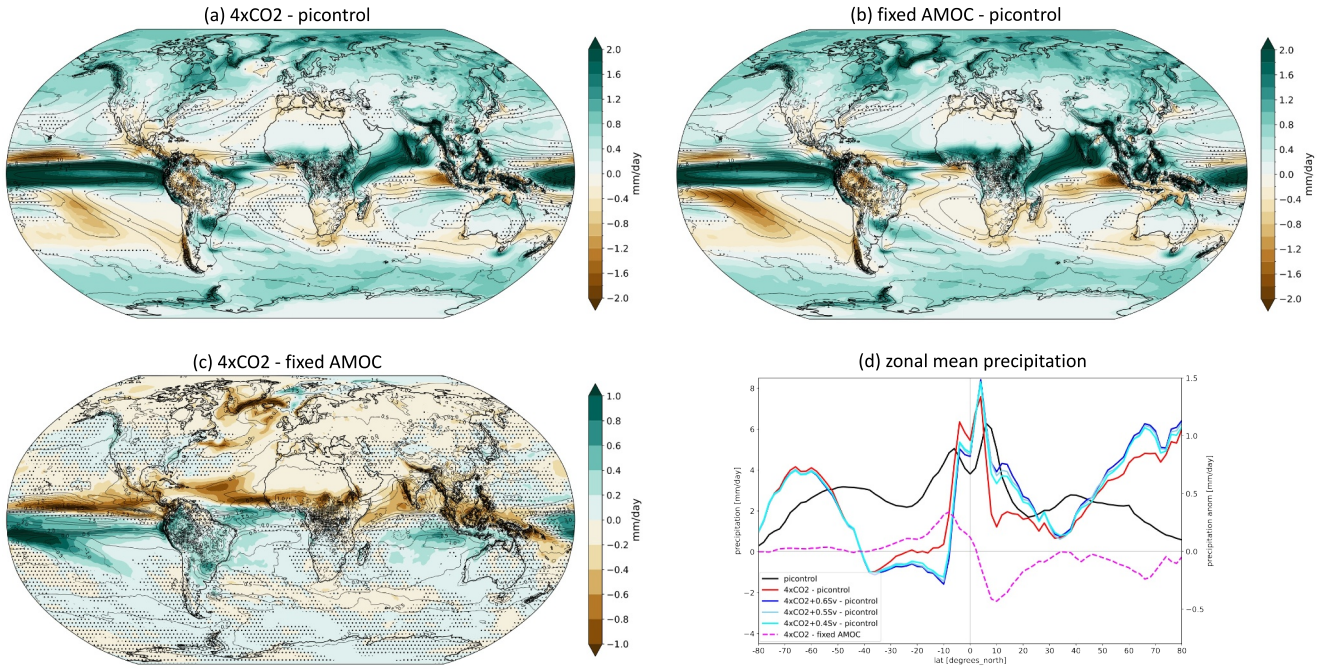


Figure 3. Precipitation. Maps show the changes in precipitation between the 4×CO_2 and picontrol (panel a), fixed Atlantic Meridional Overturning Circulation (AMOC) and picontrol (panel b), 4×CO_2 and fixed AMOC (panel c). Solid contours in panels (a) and (b) represent the climatological annual mean precipitation computed from the picontrol simulation, while in panel (c) contours show the 4×CO_2 minus picontrol anomalies. Stippling in panel (c) shows areas where the difference is not statistically significant. Panel (d) shows zonal annual mean precipitation: the black curve represents the picontrol climatology (refers to left hand side *y*-axis); the four solid curves represent changes from the picontrol (see legend); the dashed magenta curve represents the differences between the 4×CO_2 and fixed AMOC experiments.

3.4. State-Dependent AMOC Impacts

In the previous two sections we discussed temperature and precipitation impacts of a weakened AMOC relative to 4×CO_2 forcing, which we were able to separate thanks to our targeted experiments with positive virtual salinity flux. In typical CMIP6 coordinated experiments this is not possible because of other varying forcings, in addition to the AMOC decline. To overcome this, historically, AMOC impacts have been assessed with water hosing experiments starting from a preindustrial climate background. The goal of water hosing experiments was to evaluate the climate impacts arising from an artificially imposed AMOC decline in the absence of other forcings. Some of the changes that we presented so far, may appear indeed quite similar to the results of water hosing experiments, but here we are going to specifically investigate whether the impacts of an AMOC decline quantified from a water hosing experiment can be extrapolated to assess the impacts of an AMOC decline in the context of future climate change.

In Figure 4 we formally investigate the state-dependence of AMOC impacts. The top row of Figure 4 (same as Figures 2c and 3c) shows the estimated AMOC impact on temperature and precipitation in a 4×CO_2 forced climate, computed as the difference between 4×CO_2 and fixed AMOC experiments. Instead, the middle row shows changes computed from the water hosing experiment and represents the estimated AMOC impact on temperature and precipitation in a 4×CO_2 forced climate, extrapolated from the water hosing experiment (see methods). The bottom row of Figure 4 shows the differences between the top and middle rows, and quantifies the role of the background climate state on the estimates of AMOC decline impacts. If we were able to predict AMOC impacts in a 4×CO_2 climate using water hosing experiments from a preindustrial climate, then the bottom row of Figure 4 would roughly be zero everywhere. Clearly, this is not the case and the background climate state does modify both temperature and precipitation impacts of an AMOC decline, although some local impacts may be sensitive to the scaling we used to compare the experiments.

For temperature (Figure 4e), we note that the water hosing experiment would predict a much stronger cooling, especially in the mid- and high-latitude oceans. Averaged over the NH, the cooling due to a ~43% AMOC decline would be 0.7°C with a 4×CO_2 background climate, but more than twice as large (1.8°C) with a preindustrial

19448007, 2024, 10, Downloaded from https://agupubs.onlinelibrary.wiley.com/doi/10.1029/2023GL107624 by Politecnico Di Torino Sist. Bibl Del Polit Di Torino, Wiley Online Library on [13/05/2024]. See the Terms and Conditions (https://onlinelibrary.wiley.com/terms-and-conditions) on Wiley Online Library for rules of use; OA articles are governed by the applicable Creative Commons License

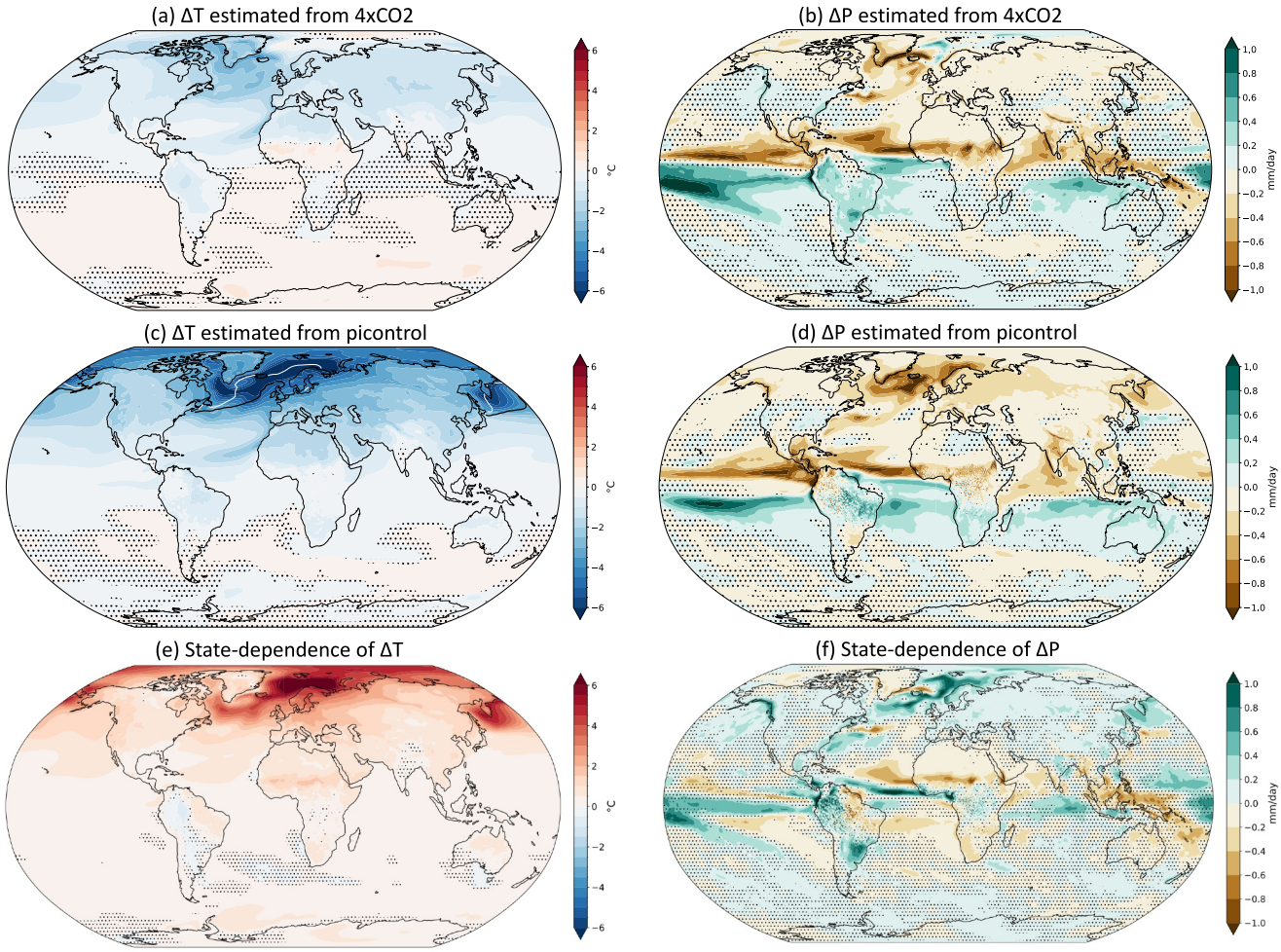


Figure 4. Background state dependence of Atlantic Meridional Overturning Circulation (AMOC) impacts. Top row panels show the change in near-surface air temperature and precipitation due to a weakened AMOC in a 4×CO_2 forced climate. They are computed as differences between the 4×CO_2 and fixed AMOC (same as Figures 2c and 3c, respectively). Middle row panels show the change in near-surface air temperature and precipitation extrapolated from the water hosing experiment with a preindustrial climate background (see scaling described in the text). Bottom row panels show the difference between of the top panels and the middle panels. Thick contours in panel (c) indicate the northern hemisphere sea ice edge in March for picontrol (white) and water hosing (black). Stippling indicates areas where differences are not statistically significant.

climate. Regionally, the SPNA cools by 2.4°C in the 4×CO_2 background climate compared to 4.9°C in a preindustrial climate. The ice-albedo feedback provides a plausible physical mechanism for these differences: as the sea ice edge in the picontrol is located within the SPNA (see contours in Figure 4c), expanding sea ice provides a positive feedback that enhances cooling in the water hosing experiments, but is absent in the almost ice-free 4×CO_2. Overall, the impact of an AMOC decline on temperature in a 4×CO_2 climate is smaller than it would be in a preindustrial climate state, although still quite large in certain regions (Figure 4a), such as the North Atlantic. An important point here is that, differently from a preindustrial climate where a weaker AMOC promotes more sea ice, an AMOC decline does not offset sea ice melting in a 4×CO_2 climate, except in some limited regions (Figure S6 in Supporting Information S1).

The state-dependence of AMOC impacts on precipitation change is less uniform in space and also exhibits regions of zonal asymmetries. Precipitation impacts are only significant in some regions, mainly the mid-latitudes in the NH, the North Atlantic and Arctic, and the tropics. At high latitudes, the water hosing would predict more drying than with the 4×CO_2 climate background state, presumably also related to an ice-free ocean in a 4×CO_2 climate that allows for more evaporation and precipitation. Very different from the water hosing extrapolation is the tropical Pacific precipitation response: in the 4×CO_2 climate state, the AMOC decline promotes an El-Niño like precipitation pattern with reduced precipitation over the western equatorial Pacific and enhanced precipitation

19448007, 2024, 10, Downloaded from https://agupubs.onlinelibrary.wiley.com/doi/10.1029/2023GL107624 by Politecnico Di Torino Sist. Bibl Del Polit Di Torino, Wiley Online Library on [13/05/2024]. See the Terms and Conditions (https://onlinelibrary.wiley.com/terms-and-conditions) on Wiley Online Library for rules of use; OA articles are governed by the applicable Creative Commons License

over the central and eastern Pacific. Instead, the water hosing extrapolation (Figure 4d) shows no significant influence over the equatorial Pacific.

We note important differences also in the Western Pacific: while the weaker AMOC in the $4\times CO_2$ background climate reduces precipitation and has no significant changes over Australia, the weaker AMOC in the preindustrial climate shows small anomalies in the Western Pacific and increased precipitation over Australia. These changes seem to be related to the southward shift of the ITCZ in the water hosing experiment, while they are affected by changes in the tropical Pacific in the $4\times CO_2$ fixed AMOC experiments. Some patterns of precipitation change may be model dependent (Timmermann et al., 2007) and could also be related to regional changes in meridional gradients of tropical SST anomalies (cf. Good et al., 2022).

4. Conclusion

Our understanding of AMOC decline impacts on future climate change is challenged by the uncertainty in past reconstructions of AMOC strength and impacts (e.g., Caesar et al., 2021; Kilbourne et al., 2022), and the inter-model spread in the AMOC response to greenhouse gas forcing in idealized simulations of future climate change (e.g., Bellomo et al., 2021; Weijer et al., 2020). Therefore, specific numerical simulations are needed to isolate the global climate response to AMOC decline. Several prior studies have carried out the so-called "water hosing" model experiments to investigate the impacts of an abrupt AMOC shutdown (e.g., Jackson et al., 2015). These studies have also helped us understand the role of AMOC in past climate changes, and probe the sensitivity of AMOC as a potential tipping element in the climate system (Weijer et al., 2019). However, studies that performed experiments targeting AMOC impacts in future climate change are limited (Liu et al., 2020; Vellinga & Wood, 2008).

In this study, we performed targeted model simulations to investigate the climate impacts of a weakened AMOC in a $4\times CO_2$ forced climate. We showed that an AMOC weakening of ~10 Sv leads a reduction in NH temperature warming, widespread NH drying and a southward shift of the ITCZ, in agreement with Liu et al. (2020). We further demonstrated that AMOC impacts depend on the background climate state for at least two fundamental climate variables: near-surface temperature and precipitation. Our results show that caution should be taken to quantify the impacts of AMOC decline under future climate change scenarios. For example, the interaction of the AMOC with other potential tipping elements (e.g., Wunderling et al., 2021) and with the global water cycle (Douville et al., 2021) has sometimes been derived from preindutrial water hosing simulations. However, our results indicate that these impacts cannot be simply extrapolated: instead, they should be quantified taking into account the warming background climate in the future. In fact, due to sea ice feedbacks, water hosing experiments would overestimate the cooling due to a weakened AMOC in a $4\times CO_2$ climate. In addition, we found that water hosing experiments would also overestimate the drying in the NH, and do not show an equatorial Pacific El Niño-like precipitation change in our model.

One important caveat of our study is that we used only one climate model, and it would be worth corroborating our findings with coordinated model inter-comparisons. For example, regional patterns of precipitation change may be influenced by the exact amount of AMOC weakening, and also exhibit substantial inter-model differences (cf. Liu et al., 2020; Good et al., 2022; Timmermann et al., 2007). We also investigated a quite abrupt and strong CO_2 forcing, which allowed us to examine changes in a rather long (100 years) quasi-equilibrium state, but did not allow us to assess transient AMOC impacts in a more realistic 21st century climate scenario. In conclusion, we suggest that important insights can be gained from similar experiments with other models. In addition, other useful experimental designs could include ramping up/down the greenhouse gas forcing or the salinity flux, to further explore the AMOC sensitivity to forcing.

Acknowledgments
KB received funding from the European Union's Horizon 2020 research and innovation programme under the Marie Skłodowska-Curie Grant agreement no. 101026907 (CliMOC). OM received funding under the Marie Skłodowska-Curie Grant agreement no. 956170 (CriticalEarth). The simulations shown in this work were carried out at ECMWF under the special projects SPITBELL and SPITMEHL.

Data Availability Statement

A dataset to reproduce the figures in this article may be found here: Bellomo and Mehling (2023).

References

Balsamo, G., Beljaars, A., Scipal, K., Viterbo, P., vanden Hurk, B., Hirschi, M., & Betts, A. K. (2009). A revised hydrology for the ECMWF model: Verification from field site to terrestrial water storage and impact in the integrated forecast system. *Journal of Hydrometeorology*, *10*(3), 623–643. https://doi.org/10.1175/2008JHM1068.1

19448007, 2024, 10, Downloaded from https://agupubs.onlinelibrary.wiley.com/doi/10.1029/2023GL107624 by Politecnico Di Torino Sist. Bibl Del Polit Di Torino, Wiley Online Library on [13/05/2024]. See the Terms and Conditions (https://onlinelibrary.wiley.com/terms-and-conditions) on Wiley Online Library for rules of use; OA articles are governed by the applicable Creative Commons License

Bellomo, K., Angeloni, M., Corti, S., & von Hardenberg, J. (2021). Future climate change shaped by inter-model differences in Atlantic meridional overturning circulation response. *Nature Communications*, *12*(1), 3659. https://doi.org/10.1038/s41467-021-24015-w

Bellomo, K., Meccia, V. L., D'Agostino, R., Fabiano, F., Larson, S. M., von Hardenberg, J., & Corti, S. (2023). Impacts of a weakened AMOC on precipitation over the Euro-Atlantic region in the EC-Earth3 climate model. *Climate Dynamics*, *61*(7–8), 3397–3416. https://doi.org/10.1007/s00382-023-06754-2

Bellomo, K., & Mehling, O. (2023). Dataset for "Impacts and state-dependence of AMOC weakening in a warming climate" by Bellomo and Mehling [Dataset]. *Zenodo*. https://zenodo.org/records/10277438

Bellomo, K., Murphy, L. N., Cane, M. A., Clement, A. C., & Polvani, L. M. (2018). Historical forcings as main drivers of the Atlantic multi-decadal oscillation in the CESM large ensemble. *Climate Dynamics*, *50*(9–10), 3687–3698. https://doi.org/10.1007/s00382-017-3834-3

Brayshaw, D. J., Woollings, T., & Vellinga, M. (2009). Tropical and extratropical responses of the North Atlantic atmospheric circulation to a sustained weakening of the MOC. *Journal of Climate*, *22*(11), 3146–3155. https://doi.org/10.1175/2008jcli2594.1

Buckley, M. W., & Marshall, J. (2016). Observations, inferences, and mechanisms of the Atlantic meridional overturning circulation: A review. *Reviews of Geophysics*, *54*(1), 5–63. https://doi.org/10.1002/2015RG000493

Caesar, L., McCarthy, G. D., Thornalley, D. J. R., Cahill, N., & Rahmstorf, S. (2021). Current Atlantic meridional overturning circulation weakest in last millennium. *Nature Geoscience*, *14*(3), 118–120. https://doi.org/10.1038/s41561-021-00699-z

Chen, D., Rojas, M., Samset, B. H., Cobb, K., Diongue Niang, A., Edwards, P., et al. (2021). Framing, context, and methods. In V. Masson-Delmotte, P. Zhai, A. Pirani, S. L. Connors, C. Péan, S. Berger, et al. (Eds.), *Climate change 2021: The physical science basis. Contribution of working group I to the sixth assessment report of the intergovernmental panel on climate change* (pp. 147–286). Cambridge University Press. https://doi.org/10.1017/9781009157896.003

Craig, A., Valcke, S., & Coquart, L. (2017). Development and performance of a new version of the OASIS coupler, OASIS3-MCT_3.0. *Geoscientific Model Development*, *10*(9), 3297–3308. https://doi.org/10.5194/gmd-10-3297-2017

Döscher, R., Acosta, M., Alessandri, A., Anthoni, P., Arsouze, T., Bergman, T., et al. (2022). The EC-Earth3 Earth system model for the coupled model intercomparison project 6. *Geoscientific Model Development Discussions*, *15*(7), 2973–3020. https://doi.org/10.5194/gmd-15-2973-2022

Douville, H., Raghavan, K., Renwick, J., Allan, R. P., Arias, P. A., Barlow, M., et al. (2021). Water cycle changes. In V. Masson-Delmotte, P. Zhai, A. Pirani, S. L. Connors, C. Péan, S. Berger, et al. (Eds.), *Climate change 2021: The physical science basis. Contribution of working group I to the sixth assessment report of the intergovernmental panel on climate change* (pp. 1055–1210). Cambridge University Press. https://doi.org/10.1017/9781009157896.010

Eyring, V., Bony, S., Meehl, G. A., Senior, C. A., Stevens, B., Stouffer, R. J., & Taylor, K. E. (2016). Overview of the coupled model intercomparison project Phase 6 (CMIP6) experimental design and organization. *Geoscientific Model Development*, *9*(5), 1937–1958. https://doi.org/10.5194/gmd-9-1937-2016

Feulner, G., Rahmstorf, S., Levermann, A., & Volkwardt, S. (2013). On the origin of the surface air temperature difference between the hemispheres in Earth's present-day climate. *Journal of Climate*, *26*(18), 7136–7150. https://doi.org/10.1175/JCLI-D-12-00636.1

Fox-Kemper, B., Hewitt, H. T., Xiao, C., Aðalgeirsdóttir, G., Drijfhout, S. S., Edwards, T. L., et al. (2021). Ocean, cryosphere and sea level change. In V. Masson-Delmotte, P. Zhai, A. Pirani, S. L. Connors, C. Péan, S. Berger, et al. (Eds.), *Climate change 2021: The physical science basis. Contribution of working group I to the sixth assessment report of the intergovernmental panel on climate change* (pp. 1211–1362). Cambridge University Press. https://doi.org/10.1017/9781009157896.011

Frierson, D., Hwang, Y. T., Fučkar, N. S., Seager, R., Kang, S. M., Donohoe, A., et al. (2013). Contribution of ocean overturning circulation to tropical rainfall peak in the Northern Hemisphere. *Nature Geoscience*, *6*(11), 940–944. https://doi.org/10.1038/ngeo1987

Good, P., Boers, N., Boulton, C. A., Lowe, J. A., & Richter, I. (2022). How might a collapse in the Atlantic meridional overturning circulation affect rainfall over tropical South America? *Climate Resilience and Sustainability*, *1*(1), e26. https://doi.org/10.1002/cli2.26

Jackson, L. C., Alastrué de Asenjo, E., Bellomo, K., Danabasoglu, G., Haak, H., Hu, A., et al. (2023). Understanding AMOC stability: The North Atlantic hosing model intercomparison project. *Geoscientific Model Development*, *16*, 1–32. https://doi.org/10.5194/gmd-2022-277

Jackson, L. C., Kahana, R., Graham, T., Ringer, M. A., Woollings, T., Mecking, J. V., & Wood, R. A. (2015). Global and European climate impacts of a slowdown of the AMOC in a high resolution GCM. *Climate Dynamics*, *45*(11–12), 3299–3316. https://doi.org/10.1007/s00382-015-2540-2

Kageyama, M., Merkel, U., Otto-Bliesner, B., Prange, M., Abe-Ouchi, A., Lohmann, G., et al. (2013). Climatic impacts of fresh water hosing under last glacial maximum conditions: A multi-model study. *Climate of the Past*, *9*(2), 935–953. https://doi.org/10.5194/cp-9-935-2013

Kang, S. M., Held, I. M., Frierson, D. M. W., & Zhao, M. (2008). The response of the ITCZ to extratropical thermal forcing: Idealized slab-ocean experiments with a GCM. *Journal of Climate*, *21*(14), 3521–3532. https://doi.org/10.1175/2007jcli2146.1

Kilbourne, K. H., Wanamaker, A. D., Moffa-Sanchez, P., Reynolds, D. J., Amrhein, D. E., Butler, P. G., et al. (2022). Atlantic circulation change still uncertain. *Nature Geoscience*, *15*(3), 165–167. https://doi.org/10.1038/s41561-022-00896-4

Latif, M., Sun, J., Visbeck, M., & Hadi Bordbar, M. (2022). Natural variability has dominated Atlantic meridional overturning circulation since 1900. *Nature Climate Change*, *12*(5), 455–460. https://doi.org/10.1038/s41558-022-01342-4

Liu, W., Fedorov, A., Xie, S.-P., & Hu, S. (2020). Climate impacts of a weakened Atlantic meridional overturning circulation in a warming climate. *Science Advances*, *6*(26), eaaz4876. https://doi.org/10.1126/sciadv.aaz4876

Lynch-Stieglitz, J. (2017). The Atlantic meridional overturning circulation and abrupt climate change. *Annual Review of Marine Science*, *9*(1), 83–104. https://doi.org/10.1146/annurev-marine-010816-060415

Madec, G. (2015). NEMO ocean engine. Note du Pole de modelisation de l'Institut Pierre-Simon Laplace No. 27.

Malmierca-Vallet, I., & Sime, L. C. (2023). Dansgaard–Oeschger events in climate models: Review and baseline Marine Isotope Stage 3 (MIS3) protocol. *Climate of the Past*, *19*(5), 915–942. https://doi.org/10.5194/cp-19-915-2023

Marshall, J., Donohoe, A., Ferreira, D., & McGee, D. (2014). The ocean's role in setting the mean position of the Inter-Tropical Convergence Zone. *Climate Dynamics*, *42*(7–8), 1967–1979. https://doi.org/10.1007/s00382-013-1767-z

Meccia, V. L., Simolo, C., Bellomo, K., & Cort, S. (2024). Extreme cold events in Europe under a reduced AMOC. *Environmental Research Letters*, *19*(1), 014054. https://doi.org/10.1088/1748-9326/ad14b0

Moffa-Sánchez, P., Moreno-Chamarro, E., Reynolds, D. J., Ortega, P., Cunningham, L., Swingedouw, D., et al. (2019). Variability in the northern North Atlantic and Arctic Oceans across the last two millennia: A review. *Paleoceanography and Paleoclimatology*, *34*(8), 1399–1436. https://doi.org/10.1029/2018PA003508

Rahmstorf, S., Box, J. E., Feulner, G., Mann, M. E., Robinson, A., Rutherford, S., & Schaffernicht, E. J. (2015). Exceptional twentieth-century slowdown in Atlantic Ocean overturning circulation. *Nature Climate Change*, *5*(5), 475–480. https://doi.org/10.1038/nclimate2554

Reintges, A., Martin, T., Latif, M., & Keenlyside, N. S. (2017). Uncertainty in twenty-first century projections of the Atlantic meridional overturning circulation in CMIP3 and CMIP5 models. *Climate Dynamics*, *49*(5–6), 1495–1511. https://doi.org/10.1007/s00382-016-3180-x

19448007, 2024, 10, Downloaded from https://agupubs.onlinelibrary.wiley.com/doi/10.1029/2023GL107624 by Politecnico Di Torino Sist. Bibl Del Polit Di Torino, Wiley Online Library on [13/05/2024]. See the Terms and Conditions (https://onlinelibrary.wiley.com/terms-and-conditions) on Wiley Online Library for rules of use; OA articles are governed by the applicable Creative Commons License

Rousset, C., Vancoppenolle, M., Madec, G., Fichefet, T., Flavoni, S., Barthélemy, A., et al. (2015). The Louvain-La-Neuve sea ice model LIM3.6: Global and regional capabilities. *Geoscientific Model Development*, *8*(10), 2991–3005. https://doi.org/10.5194/gmd-8-2991-2015

Srokosz, M., Danabasoglu, G., & Patterson, M. (2021). Atlantic meridional overturning circulation: Reviews of observational and modeling advances—An introduction. *Journal of Geophysical Research: Oceans*, *126*(1), e2020JC016745. https://doi.org/10.1029/2020JC016745

Stouffer, R. J., Yin, J., Gregory, J. M., Dixon, K. W., Spelman, M. J., Hurlin, W., et al. (2006). Investigating the causes of the response of the thermohaline circulation to past and future climate changes. *Journal of Climate*, *19*(8), 1365–1387. https://doi.org/10.1175/jcli3689.1

Timmermann, A., Okumura, Y., An, S. I., Clement, A., Dong, B., Guilyardi, E., et al. (2007). The influence of a weakening of the Atlantic meridional overturning circulation on ENSO. *Journal of Climate*, *20*(19), 4899–4919. https://doi.org/10.1175/jcli4283.1

Trenberth, K. E., Zhang, Y., Fasullo, J. T., & Cheng, L. (2019). Observation-based estimates of global and basin ocean meridional heat transport time series. *Journal of Climate*, *32*(14), 4567–4583. https://doi.org/10.1175/JCLI-D-18-0872.1

Vellinga, M., & Wood, R. (2008). Impacts of thermohaline circulation shut-down in the twenty-first century. *Climate Change*, *91*(1–2), 43–63. https://doi.org/10.1007/s10584-006-9146-y

Weijer, W., Cheng, W., Drijfhout, S. S., Federov, A. V., Hu, A., Jackson, L. C., et al. (2019). Stability of the Atlantic meridional overturning circulation: A review and synthesis. *Journal of Geophysical Research: Oceans*, *124*(8), 5336–5375. https://doi.org/10.1029/2019JC015083

Weijer, W., Cheng, W., Garuba, O., Hu, A., & Nadiga, B. (2020). CMIP6 models predict significant 21st century decline of the Atlantic meridional overturning circulation. *Geophysical Research Letters*, *47*(12), e2019GL086075. https://doi.org/10.1029/2019GL086075

Woollings, T., Gregory, J. M., Pinto, J. G., Reyers, M., & Brayshaw, D. J. (2012). Response of the North Atlantic storm track to climate change shaped by ocean–atmosphere coupling. *Nature Geoscience*, *5*(5), 313–317. https://doi.org/10.1038/ngeo1438

Worthington, E. L., Moat, B. I., Smeed, D. A., Mecking, J. V., Marsh, R., & McCarthy, G. D. (2021). A 30-year reconstruction of the Atlantic meridional overturning circulation shows no decline. *Ocean Science*, *17*(1), 285–299. https://doi.org/10.5194/os-17-285-2021

Wunderling, N., Donges, J. F., Kurths, J., & Winkelmann, R. (2021). Interacting tipping elements increase risk of climate domino effects under global warming. *Earth System Dynamics*, *12*(2), 601–619. https://doi.org/10.5194/esd-12-601-2021

Zhang, R., & Delworth, T. L. (2005). Simulated tropical response to a substantial weakening of the Atlantic thermohaline circulation. *Journal of Climate*, *18*(12), 1853–1860. https://doi.org/10.1175/JCLI3460.1

Zhang, R., Sutton, R., Danabasoglu, G., Kwon, Y.-O., Marsh, R., Yeager, S. G., et al. (2019). A review of the role of the Atlantic meridional overturning circulation in Atlantic multidecadal variability and associated climate impacts. *Reviews of Geophysics*, *57*(2), 316–375. https://doi.org/10.1029/2019RG000644

19448007, 2024, 10, Downloaded from https://agupubs.onlinelibrary.wiley.com/doi/10.1029/2023GL107624 by Politecnico Di Torino Sist. Bibl Del Polit Di Torino, Wiley Online Library on [13/05/2024]. See the Terms and Conditions (https://onlinelibrary.wiley.com/terms-and-conditions) on Wiley Online Library for rules of use; OA articles are governed by the applicable Creative Commons License